

Simulation of boundary layer characteristics using 1-D PBL model over Goa during ARMEX-I

Y. Das, U. C. Mohanty

Centre for Atmospheric Sciences, Indian Institute of Technology Delhi¹

Abstract: This paper presents the characteristic features involved in the variability of the planetary boundary layer (PBL) over Goa (15.38°N, 73.83°E), located in the west coastal belt of Indian Peninsula. This work was carried out during the Arabian Sea Monsoon Experiment (ARMEX) field campaign, which was the second observational programme under the Indian Climate Research Program (ICRP), during June-August 2002. A high-resolution sounding data comprising the vertical profiles of temperature, humidity, zonal and meridional component of wind, along the vertical, was obtained during ARMEX-I observational campaign that was used to study the PBL characteristics over Goa during convectively active and convectively suppressed episodes in June and July 2002, respectively. For this purpose a one-dimensional multi-level PBL model with a TKE- ε closure scheme was used. The temporal evolution of turbulent kinetic energy (TKE), planetary boundary layer (PBL) height, sensible and latent heat fluxes are simulated for these specific convective episodes during ARMEX-I. The model also generates the vertical profiles of potential temperature, specific humidity, zonal and meridional wind that compare reasonably well with the observations.

Key words: Arabian Sea Monsoon Experiment (ARMEX), planetary boundary layer (PBL) height, sensible and latent heat fluxes, turbulent kinetic energy (TKE)

1. Introduction

The Arabian Sea Monsoon Experiment (ARMEX) was the second observational programme under the Indian Climate Research Program (ICRP). In this observational campaign, detailed observations were made during June-August 2002 in order to study the boundary layer characteristics in different synoptic conditions and monsoonal activities over south west coastal

¹ Hauz Khas, New Delhi-110016, India; e-mail: yashvantdas@rediffmail.com

region of India (DST, 1998). Boundary layers of a monsoon region, in which a number of not yet fully understood processes of different scales interact, greatly affect the lowest levels of the atmosphere (*Holt and Raman, 1987*). Differential heating due to heating of the earth by radiative processes and to the heating of the atmosphere by latent and sensible heat fluxes play an important role in driving the atmospheric boundary layer characteristics. Influence of the Arabian Sea and its associated atmospheric features greatly influence the ocean-atmosphere coupling processes and coastal atmospheric boundary layer processes (*Holt and Raman, 1987*). *Kusuma et al. (1991)* and *Potty et al. (1997)* used PBL and a regional model with a high vertical resolution in the planetary boundary layer to simulate various atmospheric processes using different boundary layer parameterization schemes. Significant variation in boundary layer structure and associated processes over land as compared to oceans are reported, and in some cases the evaluation of the model sensitivity, have also been carried out. Moreover, during the Indian Ocean Experiment (INDOEX) and the Bay of Bengal Experiment (BOBMEX), studies on the variability of atmospheric boundary layer and related convective activity over Indian ocean regimes have been highlighted by *Basu et al. (1999)*; *Bhat et al. (2001; 2003)*; *Mohanty et al. (2002; 2003)*; *Sam et al. (2003)*. Similarly, data collected during the Barbados Oceanic and Meteorological Experiments (BOMEX), 1969 (*Holland and Rasmusson, 1973*) and the Atlantic Trade-Wind Experiment (ATEX), 1969 (*Augstein et al., 1971*) focused on the structure of the boundary layer during suppressed convection conditions. *Kloesel et al. (1989)* studied the structure of the boundary layer over a broad region of tropical Pacific using radiosonde measurements and indicated the critical role of low-level inversion in regulating convective activity. Taking the case of nonprecipitating convection in a tropical boundary layer, a detailed 3-D model studies on the aspects of atmospheric boundary layer were carried out, and results were compared with observational data by *Sommeria and Lemone (1978)*. Using data from tower and aircraft measurements along the Baltic coast in the southeast of Sweden, the vertical turbulence structure in the marine atmosphere along a shoreline has been investigated during spring or early summer, with a stably or neutrally stratified marine boundary layer usually capped by an inversion. The complex PBL characteristics and turbulence structure of the surface layer of the coastal marine environment are found

to be influenced by the state of the sea (*Tjernström and Smedman, 1993*). Based on airborne observations obtained during the Upper Spencer Gulf experiments in South Australia, *Shao et al. (1991)* investigated the structure of turbulence in a coastal boundary layer, which represents an extreme situation of horizontal inhomogeneity. PBL characteristics at Kalpakkam, east coastal stations of India has been carried out using Doppler mini-sodar by *Bagavath et al. (2005)*, and reported the land–ocean thermal contrast in association with thermal internal boundary layer formation. The studies on the processes of convective activity and rainfall characteristics over the coastal station Goa and also offshore Goa in SE Arabian Sea has been carried out during ARMEX-I observational campaigns (*Mohanty et al., 2005; Sam et al., 2005*).

However, very few studies have been made to illustrate the PBL characteristics and the related role of surface fluxes in influencing its variability during active and weak convection periods over coastal station of Indian subcontinent due to the paucity of data.

In the present study an attempt has been made to analyze the PBL characteristics during ARMEX-I, using 1-D PBL model with the aim to address the variation of structure of the boundary layer over Goa during active and weak episodes of convective activity; the influence of local factors on the growth in turbulent kinetic energy (TKE), and the effect in the planetary boundary layer (PBL) height, over a west coastal station of the Indian peninsula. In this station (Goa) upper air and surface observations were taken from 15 June – 15 August 2002, using Vaisala sondes by Indian Navy as a part of ARMEX-I, to procure high-resolution vertical profiles of temperature, specific humidity, wind speed and direction. Therefore, Goa was chosen as the location of the present study. These data sets produced very good opportunity to validate the 1-D PBL model with TKE- ϵ closure scheme over the coastal station of the Indian subcontinent. This is used to simulate the vertical profiles of zonal and meridional winds, potential temperature and specific humidity that compare well with the observations. Other surface parameters that determine PBL characteristics, such as PBL height, sensible heat flux, latent heat flux, evolution of turbulent kinetic energy (TKE) are also presented in this paper.

2. The data

During ARMEX-I, high-resolution upper air observations giving vertical profiles of temperature, humidity, zonal and meridional wind were obtained at every 12 hrs from 15 June to 15 August 2002, over Goa (15.38°N , 73.83°E) using Vaisala sondes by Indian Navy. A linear interpolation technique is used to interpolate the above cited parameters for every 50 m in the vertical profile. These data sets provide input for the 1-D model in simulating the PBL characteristics over Goa. The map showing the coastal station (Goa) is shown in Fig. 1.

Two different synoptic episodes were considered based on the surface synoptic observations (*IMD, 2002*), reanalysis of National Centres for Environmental Predictions/National Centre for Atmospheric Research (NCEP / NCAR) Outgoing Longwave Radiation (OLR) data obtained from National Oceanic and Atmospheric Administration’s (NOAA’s) Physical Science Division of Earth System Science Laboratory (<http://www.cdc.noaa.gov>) as

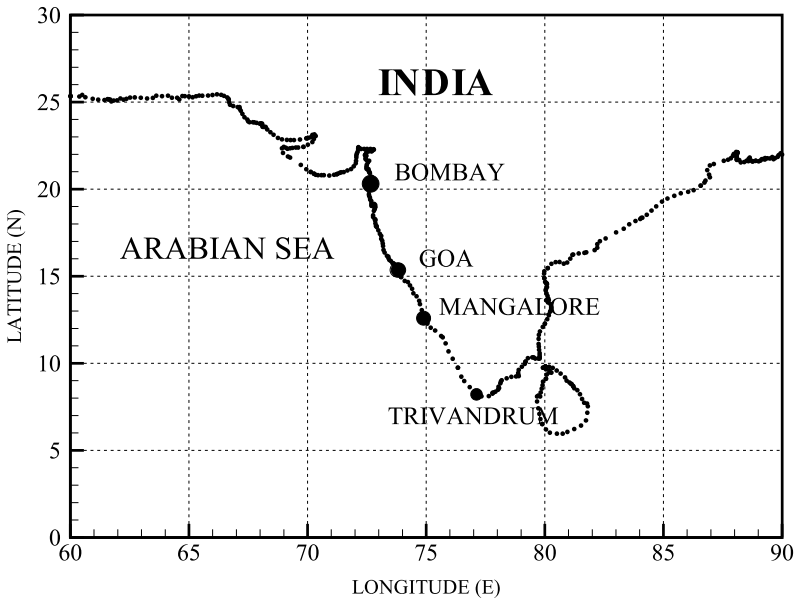


Fig. 1. Location of station Goa (15.38°N , 73.83°E) during ARMEX-I field campaign.

shown in Fig. 2 and Meteosat-7 cloud imageries (<http://www.eumetsat.int>) (Fig. 3) over Goa that was analyzed for this study (*Weather Summary ARMEX-2002; Mohanty et al., 2002*). Based on these analysis and obser-

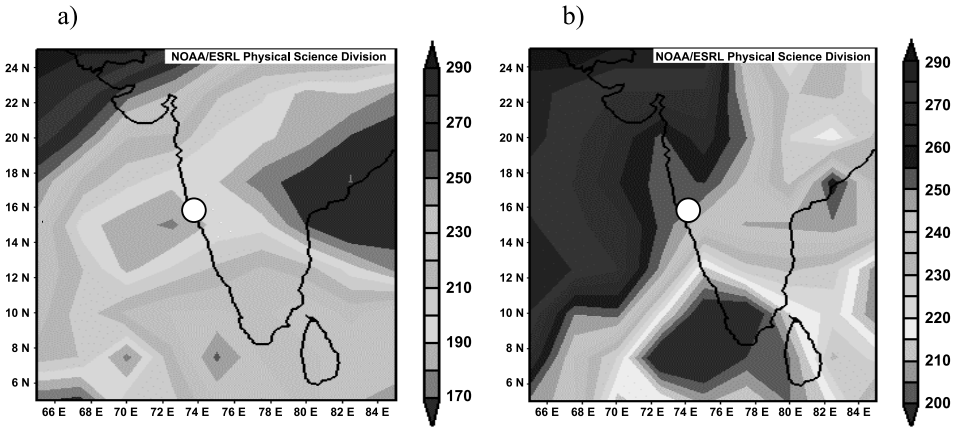


Fig. 2. Composite mean of Outgoing Longwave Radiation (OLR) (W/m^2) over Goa ($15.38^{\circ}N, 73.83^{\circ}E$) during a) 21-23 June, 2002 ($OLR < \sim 190 W/m^2$) and b) 12-14 July, 2002 ($OLR > \sim 240 W/m^2$) representing the active and suppressed convection cases, respectively.

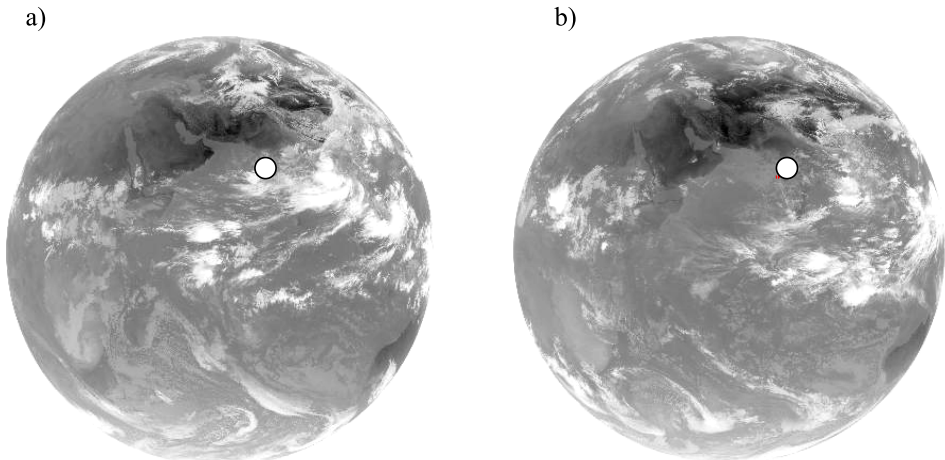


Fig. 3. Meteosat - 7 IR cloud imageries over Goa ($15.38^{\circ}N, 73.83^{\circ}E$) during (12 UTC, 22 June 2002) and (12 UTC, 13 July 2002), representing a) Active convection case and b) Suppressed convection case, respectively.

vations two specific cases were chosen over Goa cf. a) Case – I (21-23 June 2002) and b) Case – II (12-14 July 2002). Case–I is referred to as the convectively active episode. Case– II is a period where no significant convective activity noticed and is therefore called the suppressed convection event.

3. Methodology

The 1-D PBL model with TKE- ϵ closure was used to simulate the PBL characteristics during two different convective episodes considered from AR-MEX-I. The code was originally developed by *Lykossov and Platov (1992)* to simulate the PBL characteristics. The experiment has served the purpose of validating the 1-D model over the west Indian coastal station using high-resolution data.

3.1. Model

This model is a multi-level 1-D model with TKE- ϵ closure scheme. The model has 40 levels in the vertical with each layer having a uniform thickness of 50 m from surface to the top of the model (2000 m). The TKE- ϵ closure is used for the mixed layer, while the surface layer similarity approach is used for the constant flux layer close to the Land surface. *Lykossov and Platov (1992)*, *Satyanarayana et al. (1999; 2000; 2001; 2003)*, *Mohanty et al. (2002)* and *Das (2004)* give details of the model. A brief overview of the model is presented in Table 1.

In a Cartesian co-ordinate system, where the horizontal axes x and y are directed in the east and north, respectively, and the vertical axis z is directed upwards, the model solves the following equations

$$\frac{\partial u}{\partial t} = -\frac{\partial \overline{u'w'}}{\partial z} + fv + \tilde{p}_x/\tilde{\rho}, \tag{1}$$

$$\frac{\partial v}{\partial t} = -\frac{\partial \overline{v'w'}}{\partial z} - fu - \tilde{p}_y/\tilde{\rho}, \tag{2}$$

$$\frac{\partial \theta}{\partial t} + u\tilde{\theta}_x + v\tilde{\theta}_y = -\frac{\partial \overline{\theta'w'}}{\partial z} + Q_r + Q_f, \tag{3}$$

$$\frac{\partial q}{\partial t} + u\tilde{q}_x + v\tilde{q}_y = -\frac{\partial \overline{q'w'}}{\partial z} + E_p - C, \tag{4}$$

$$\frac{\partial q_w}{\partial t} + u\tilde{q}_{wx} + v\tilde{q}_{wy} = -\frac{\partial \overline{q'_w w'}}{\partial z} - E_p + C - P, \tag{5}$$

$$\frac{\partial E}{\partial t} = (-\overline{u'w'} \frac{\partial u}{\partial z} + \overline{v'w'} \frac{\partial v}{\partial z} + \frac{g}{\rho} \overline{\rho'w'} + \varepsilon) - \frac{\partial \overline{w'\varepsilon'}}{\partial z}, \tag{6}$$

$$\frac{\partial \varepsilon}{\partial t} = -C_1 \frac{\varepsilon}{b} (-\overline{u'w'} \frac{\partial u}{\partial z} + \overline{v'w'} \frac{\partial v}{\partial z} + \frac{g}{\rho} \overline{\rho'w'} + \varepsilon) - \frac{\partial \overline{w'\varepsilon'}}{\partial z}, \tag{7}$$

where

u, v and $w = x, y$ and z components of the wind velocity, respectively,

θ = the potential temperature,

q = the specific humidity,

q_w = the specific liquid-water content,

E = the turbulent kinetic energy,

ε = the dissipation,

ρ = the density of the air-water-water vapour mixture,

$(\tilde{p}_x, \tilde{p}_y), (\tilde{\theta}_x, \tilde{\theta}_y), (\tilde{q}_x, \tilde{q}_y), (\tilde{q}_{wx}, \tilde{q}_{wy})$ = components of horizontal gradients of the pressure, potential temperature, specific humidity and specific liquid-water content in the free atmosphere respectively,

fv, fu = Coriolis forces in the x and y -directions, respectively,

Q_r, Q_f = the rates of the heat change due to radiation and phase transitions of the water respectively,

C, E_p = the rates of phase changes, viz. water vapour to liquid water and water to water vapour respectively,

P = the precipitation rate,

$\overline{\rho u'w'}, \overline{\rho v'w'}, \overline{\rho \theta'w'}, \overline{\rho q'w'}$ and $\overline{\rho q'_w w'}$ = the vertical turbulent fluxes of momentum, heat, water vapour and liquid water respectively,

f = the coriolis parameter,

g = the acceleration due to gravity, and

C_1 and b are the constants.

In order to calculate vertical turbulent fluxes of momentum, heat and moisture in the interfacial layer, the Boussinesq hypothesis is used:

$$\overline{a'w'} = K_a \frac{\partial a}{\partial z}, \tag{8}$$

where a is any of the prognostic variables u, v, θ, q and q_w , and K_a is the eddy exchange coefficient. It is assumed that $K_a = \alpha_a K$, where, α_a is a dimensionless constant (equal to unity for the momentum flux). The coefficient K is related to the turbulent kinetic energy E and the dissipation rate ε following *Kolmogorov (1942)* equation:

$$K = \frac{C_k E^2}{\varepsilon}, \tag{9}$$

where, C_k is a dimensionless constant.

Table 1. Overview of the model

Model Description	One Dimensional PBL model with one and half order TKE closure scheme
Vertical Domain	2000m
Vertical Levels	40 and $\Delta Z=50$ m
Independent Variables	Z, t
Prognostic Variables	U, v, θ , q, e, ε , q_s , T_s
Diagnostic Variables	K_u , l
Numerical Scheme	Second order accuracy
Time Integration	Implicit, $\Delta t=600$ sec
Boundary Conditions	<ul style="list-style-type: none"> • Lower Boundary: Monin – Obukhov similarity theory • Upper Boundary: The Geostrophic conditions; Observed values at 1958m • TKE and ε: zero energy flux at 1958m • Under the Surface: Soil heat and moisture diffusion processes are considered
Physical Processes	<ol style="list-style-type: none"> 1. Dry and Moist Convective Adjustment 2. Sensible and latent heat fluxes 3. Fluxes under stormy conditions 4. Long-wave and short-wave radiation fluxes

4. Model initial conditions and numerical experiments

The model initial and boundary conditions are prepared from the data comprising of high-resolution observational data obtained over Goa using Vaisala sonde. The high-resolution upper air data consisting of zonal and meridional wind components, potential temperature and specific humidity are linearly interpolated to obtain the initial values at the model grid

points. These parameters that are interpolated at every 50 m in the vertical to 2000 m (top of the model domain) are taken as input to the model. The maximum height of the turbulent boundary layer (top of the PBL) is chosen as the upper boundary. At the top of the boundary layer, the wind speeds, the potential temperature and the moisture attain the observed values at that height. The TKE and energy dissipation is assumed to vanish at that height. Surface observations obtained at the same location are used for preparing the lower boundary conditions. Climatological ozone data are prescribed for the radiation parameterization scheme. For active convection case (21-23 June 2002), initial conditions are prepared from the observations at 12 hrs of 22 June 2002 and the model was integrated for 60h and for the convectively suppressed case (12-14 July 2002), the initial conditions are prepared at 12 hrs of 12 July 2002 and model integration are performed for 48 h.

The time step of integration of the model is 600 s and hourly simulation output of the model are stored for analysis and comparison with the observations.

5. Results and discussion

The 1-D model simulated vertical profiles of zonal (u) and meridional (v) wind components, potential temperature (θ) and specific humidity (q) over Goa are presented here. The observed profiles of u and v wind components, θ and q were linearly interpolated in the vertical and the resultant values (at every 50 m interval up to 2000 m) used. The diurnal variation of the fluxes of sensible heat (H) and latent heat (LE), planetary boundary layer (PBL) height, and the evolution of the TKE are illustrated for both the cases. These model outputs are compared with the observations wherever available.

5.1. H, LE and PBL Height

During the active convection periods (case-I, June 21-23, 2002) India Meteorological Department (IMD) recorded a fair amount of rainfall over

the study region, whereas no significant rainfall was recorded during suppressed convection case (12–14 July, 2002), (case-II) (IMD, 2002). *Bhat et al. (2002)* have documented that the condensation of water vapour in cumulonimbus clouds is one of the most important processes, which bring about rainfall during the convective active episodes, and latent heat release during condensation increases the temperature of the column of air from surface to the troposphere.

The diurnal variation of the surface layer fluxes of H, LE and PBL height are presented in Fig. 4a–f, for both the case-I and case-II, respectively. Diurnal variations of H and LE during both the cases (convectively active and convectively suppressed) are pronounced. During active case it is noticed from the Fig. 4a that between 11 UTC of 21 and 22 June 2002, H is lower in values when the rainfall occurred (*IMD, 2002*). Peak value of H has been simulated at ~ 06 UTC of 23 June, 2002 amounting to $\sim 37.41 \text{ W/m}^{-2}$, and then again it has lower values of $\sim -15 \text{ W/m}^2$ at ~ 23 UTC of 23 June, 2002. During case-II, H has the higher values between 2 UTC to 11 UTC of 13 July 2002 amounting to $\sim 20.18 \text{ W/m}^2$ (maximum) Fig. 4d. At around 3 UTC of 14 July lower values of H are simulated, again it has the higher values of $\sim 10.80 \text{ W/m}^2$ around 10 UTC of 14 July 2002.

The LE showed almost similar trend as that of H. The LE is in decreasing spree between 11 UTC of 21 and 22 June 2002 during the active convection case. Lower values of $\sim 6.88 \text{ W/m}^2$ are simulated at around 11 UTC of 22 June, 2002. During this episode maximum values of LE simulated are 186.82 W/m^2 between 6 to 12 UTC of June 2002 (Fig. 4b). During the suppressed convection case it shows a maximum of 85.52 W/m^2 and as low as 0 W/m^2 , Fig. 4e. Both the H and LE show higher values during case-I as compared to the case-II.

Thus simulated surface conditions are in general agreement with the relevant synoptic conditions.

The surface fluxes simulated in the boundary layer greatly modulate the PBL height. In the model, the PBL height is taken as the model level for which the turbulence ceases in the vertical for the TKE closure scheme. Fig. 4c–f shows simulated PBL height vs time (UTC) plot. The variation of PBL height is consistent with the variation of H. Case-I has a higher PBL height (maximum 1200 m) as compared to case-II (maximum 800 m). PBL height variation is not as systematic as the surface variables. There is some

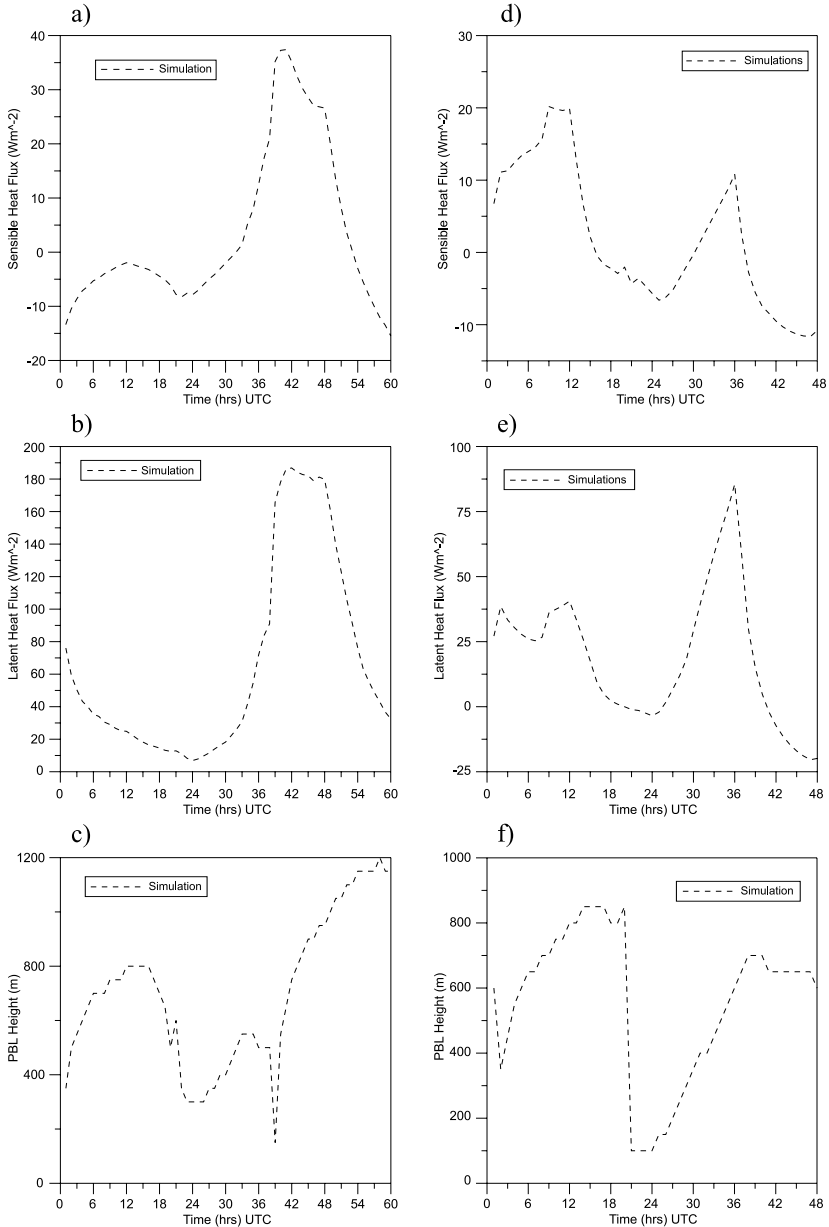


Fig. 4. Diurnal variations of a) Sensible heat flux (H), b) Latent heat flux (LE) and c) Planetary boundary layer height (PBL) height for case-I and d), e) and f) represent the variation for the same parameters for case-II, respectively.

discrepancy in the variation of PBL height with surface fluxes. This could be due to the influence of circulation and advection. The non-homogeneity of the coastal case could also be attributed to this discrepancy, which could not be resolved by 1-D model.

5.2. Evolution of TKE

The TKE variation in the lower layer of the atmosphere plays a dominant role. TKE is taken as a measure of turbulence intensity in the boundary layer, and is responsible for various boundary layer processes, such as entrainment, stability and effective transport under low wind conditions (*Satyanarayana et al., 2001*). Fig. 5a shows the evolution of the TKE with time [21 (11 UTC) - 23 (23 UTC) June 2002] during case-1. TKE has the higher values during case-I as compared to case-II (suppressed convection case), as expected. The TKE simulations (1-D) could capture the highly turbulent boundary layer rising to a height nearing 1150 m with maximum TKE value of $\sim 1.16 \text{ m}^2\text{s}^{-2}$ ($\sim 11 \text{ UTC}$, 23 June 2002). This could be due to high sensible heating, and hence turbulence generation due to both the buoyancy and shear. Shear term represents the interaction of the turbulent momentum flux with mean vertical wind shear that generates turbulence.

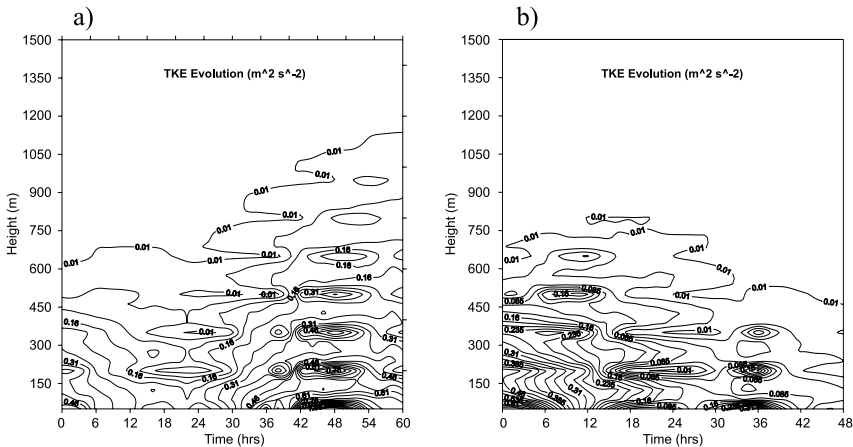


Fig. 5. Time evolution of Turbulent Kinetic Energy (TKE). a) Case-I and b) Case-II.

If carefully noticed (not shown), this term is very large ($\sim 2.5 \text{ m}^2\text{s}^{-1}$) and positive near the ground in case-I the convectively active event. This term is obviously going to be larger on windy conditions (larger vertical shear). Maximum buoyancy contribution simulated was $\sim 0.77 \text{ m}^2\text{s}^{-1}$ during the active convection period (not shown). The results are in conformity with the values reported by *Warrior (1999)* and *Satyanarayana et al. (2001)*.

During the suppressed convection period [12 (22 UTC)-14 (22UTC) July 2002] (case-2), a reduction in the evolution of TKE is noticed. The maximum TKE simulated is as low as $\sim 0.68 \text{ m}^2\text{s}^{-2}$ at around 03 UTC, 13 July 2002, (Fig. 5b), while mechanical generation, as well as the buoyancy production (not shown), too, are comparably smaller than case-I with maximum of $\sim 1.5 \text{ m}^2\text{s}^{-1}$ and $0.29 \text{ m}^2\text{s}^{-1}$, respectively, below 300 m in the vertical. The conditions observed during this period are almost a statically stable atmosphere, where an air parcel displaced vertically by turbulence would experience a buoyancy force pushing it back towards its starting height. Thus the static stability suppresses the TKE. The variability of TKE evolutions in both the cases are greatly influenced by the wind condition and shear production, though the sensible heating can add to the TKE production through buoyancy, which is comparatively lower than shear production for TKE generation (*Sam et al., 2003*).

5.3. Validation of the 1-D model

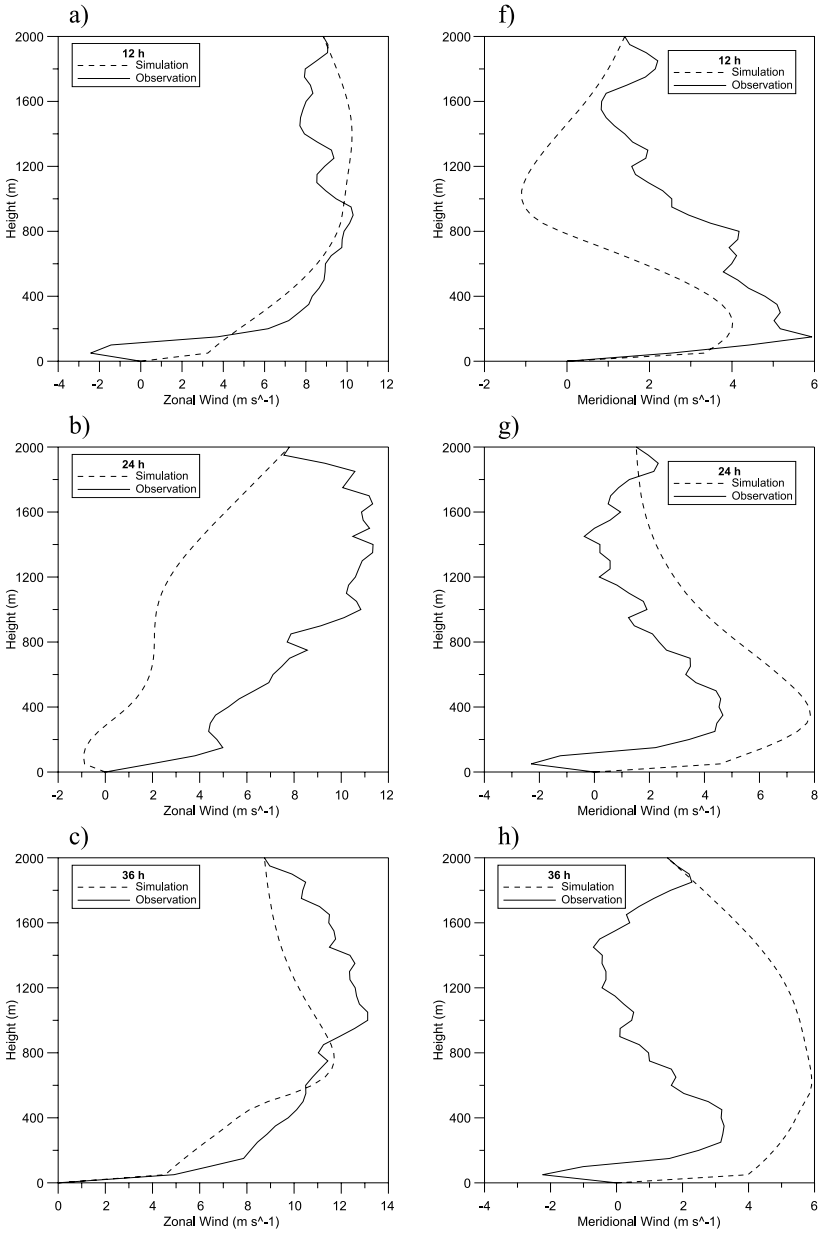
Figs. 6a-j and 7a-j represent the 1-D simulation of u, v, θ and q profiles for case-I (21-23 June, 2002). Case-II (12 -14 July, 2002) is represented by Figs. 8a-h and 9a-h. Although hourly simulations are available, only representative profiles are shown, for which observations are available. The simulations given in Figs. 6a-j and 7a-j are at 23 UTC (21 June, 2002), 11 UTC (22 June, 2002), 23 UTC (22 June, 2002), 11 UTC (23 June, 2002) and 23 UTC (23 June, 2002). They correspond to 12 h, 24 h, 36 h, 48 h and 60 h of simulations, with initial values at 11 UTC of 21 June 2002. Similarly, the representative profiles with figures as shown and mentioned for case-II, are at 11 UTC (13 July, 2002), 24 UTC (13 July, 2002), 10 UTC (14 July, 2002) and 22 UTC (14 July, 2002) and correspond to 13h, 26h, 36h and 48h of simulations, respectively; initialized at 22 UTC of 12 July 2002 in this case.

Considering a general overview of the simulation, it is clear from Figs. 6a-j, 7a-j, 8a-h and 9a-h that almost all the simulated profiles for both the cases compare well with the observed profiles irrespective of the large variation observed in the synoptic conditions. Although the u and v wind components show few aberrations from the observations, as obvious from the simulated profiles shown in the Figs. 6a-j and 8a-h, they follow the same trend. This could be due to the limitations that are encountered in a 1-D model to simulate all the processes active for any given scenario due to non-homogeneity and advection. The simulated θ profiles are in a fairly good agreement during both the synoptic situations considered in this study (Figs. 7a-j and 9a-h). There is a slight under-prediction ($2-3 \text{ gkg}^{-1}$) in the q profile at 60 h simulation during case-I, as is obvious from Fig. 7j. However, the simulated humidity profiles show good agreement with the observed profiles. It is evident from the figures that the simulated profiles are in good agreements with observations, though the quantitative values are different. The study reveals that the thermodynamic structure was better simulated than the dynamical fields in the 1-D simulation. However, the overall performance of the 1-D PBL model was fairly promising.

To quantify the model's ability to replicate observations, a simple statistical evaluation is undertaken. The correlation coefficient and root mean square (RMS) error at different simulation hours with respect to observations for case-I and case-II are computed and presented in Table 2. Much of the statistics is in agreement with the discussion above. The RMS error of zonal and meridional winds are found to be comparatively less for case-II than for case-I, though they are fairly correlated with the observations. In both the cases the simulated profiles of θ and q show a reasonably good agreement with the observations.

6. Conclusions

A multi-level 1-D PBL model was applied during the observational programme ARMEX-I to the active and suppressed convection episodes. The model was able to capture the main characteristic features of these two synoptic situations. The following broad conclusions could be drawn from the results of the numerical simulations. Higher values of H and LE are noticed



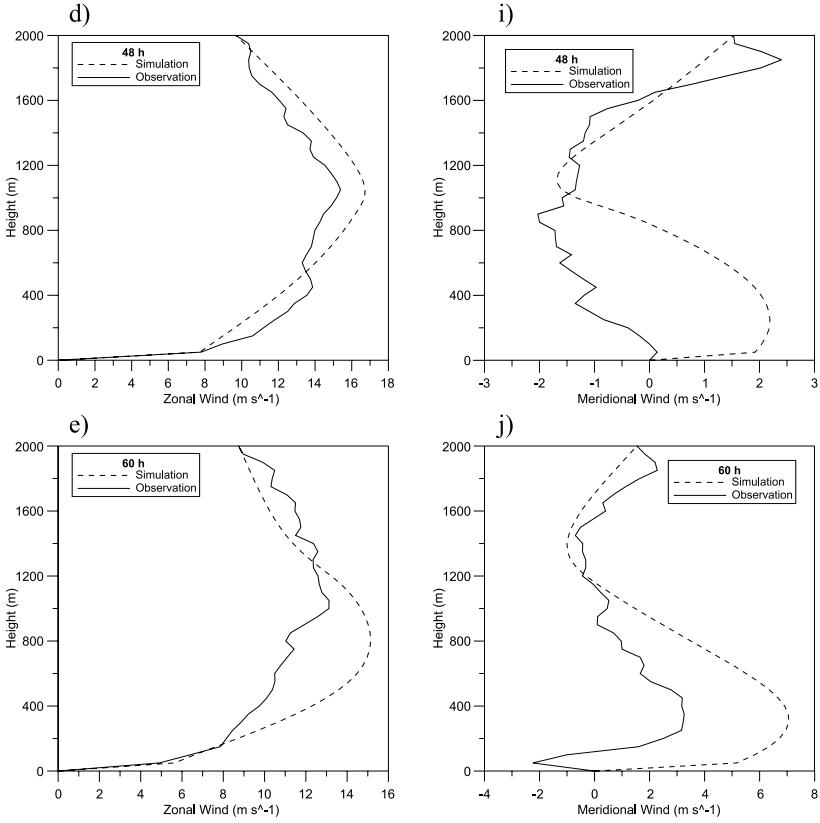
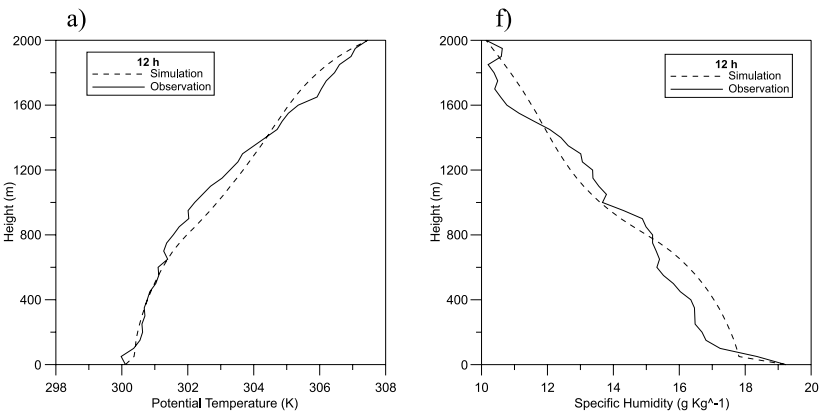
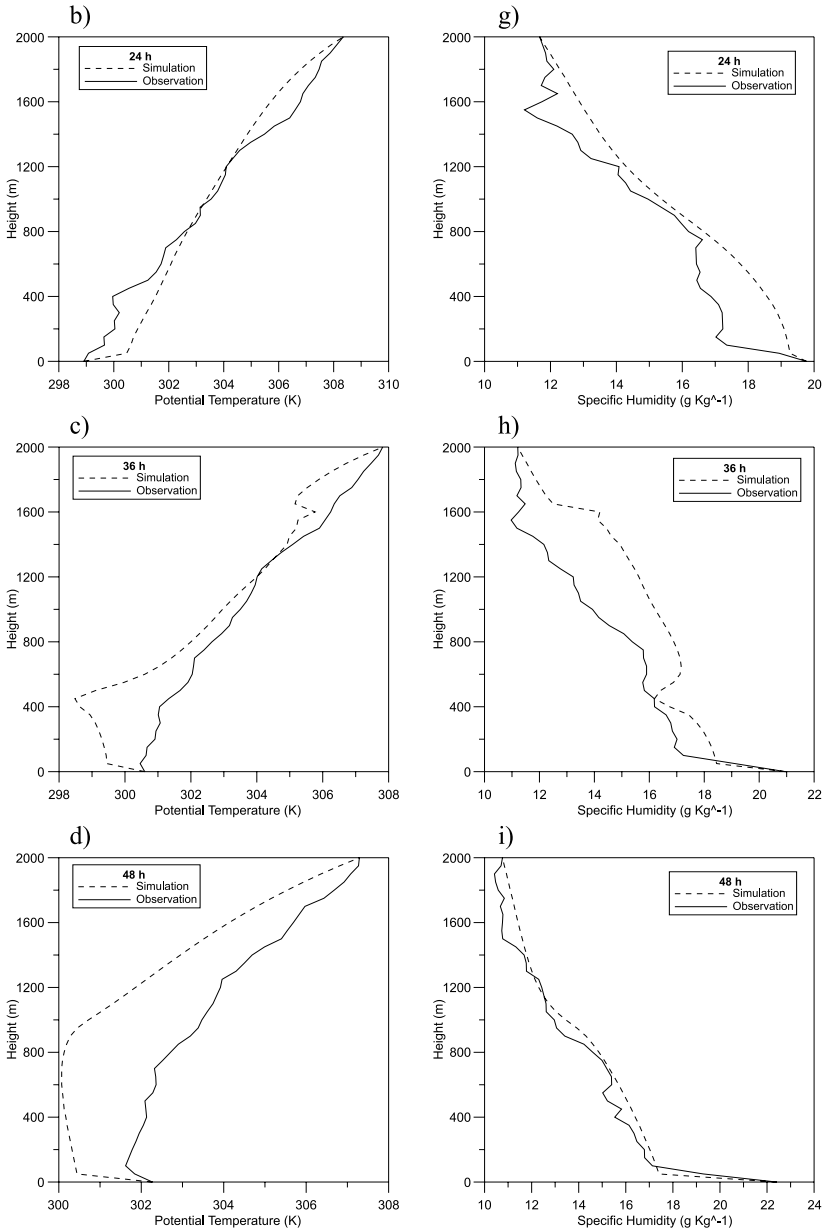


Fig. 6a-j. Vertical profiles of simulated and observed zonal wind (u) and meridional wind (v) fields for different representative hours of simulations for case-I.





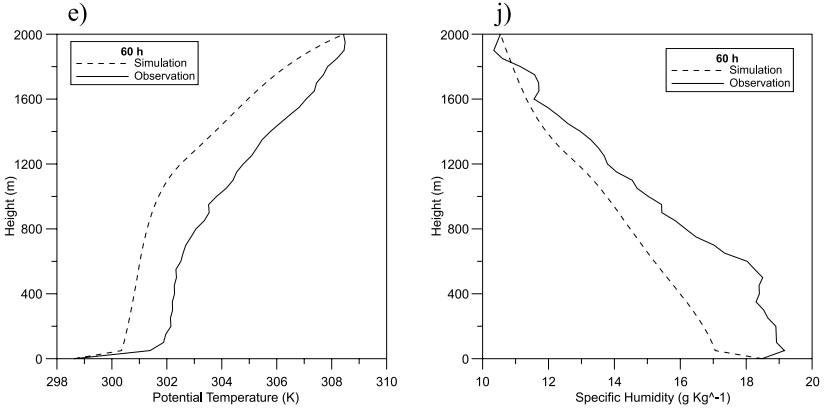
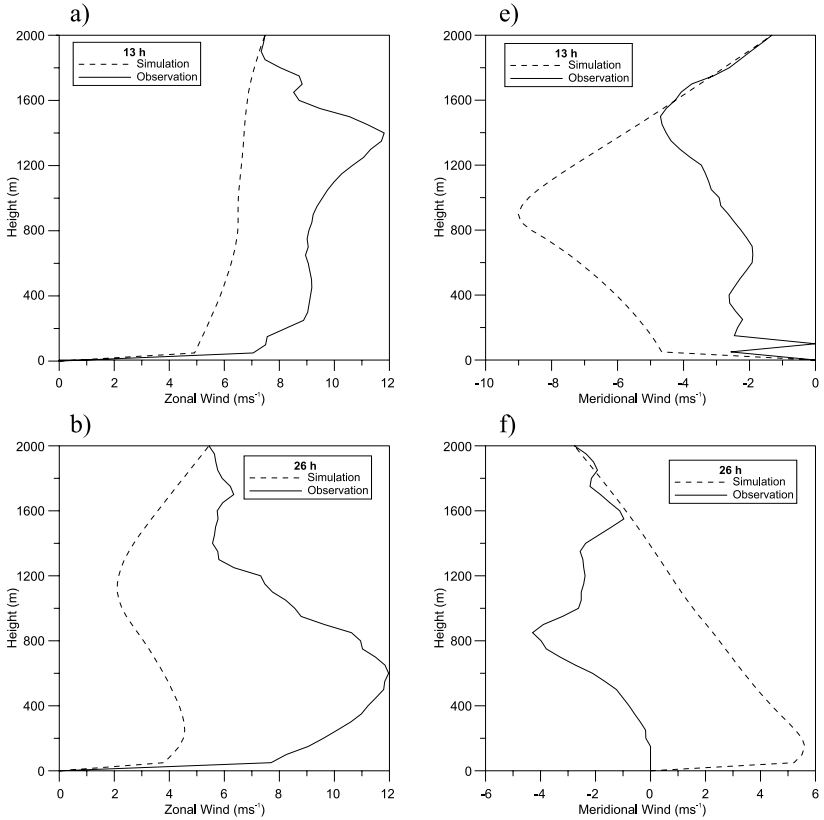


Fig. 7a-j. Vertical profiles of simulated and observed potential temperature (θ) and specific humidity (q) for different hours of simulations for case-I.



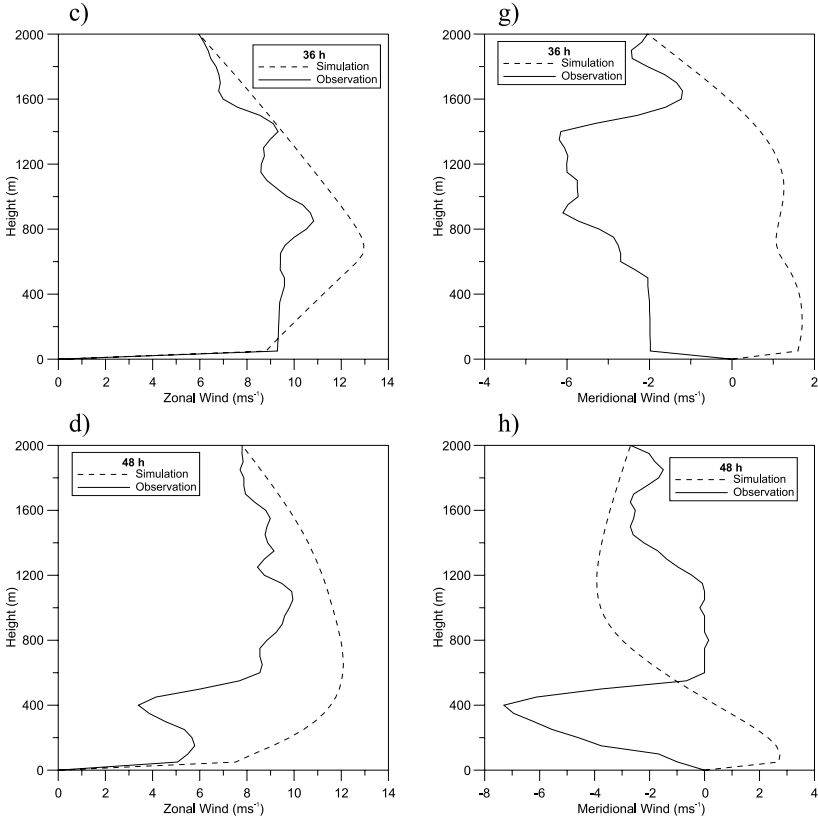
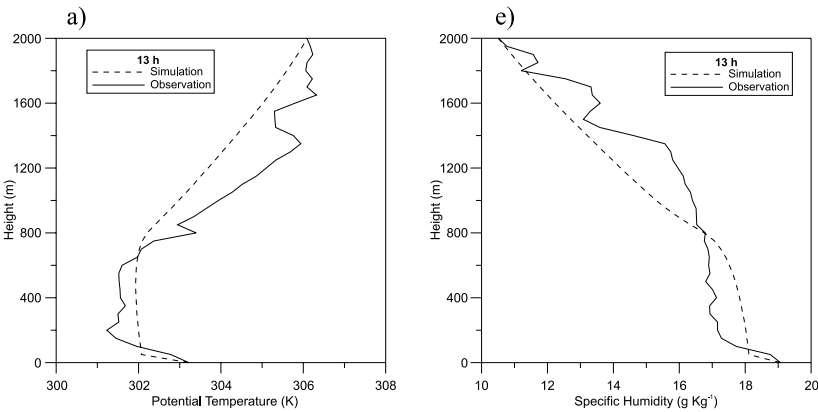


Fig. 8a-h. Vertical profiles of simulated and observed zonal wind (u) and meridional wind (v) fields for different hours of simulations for case-II.



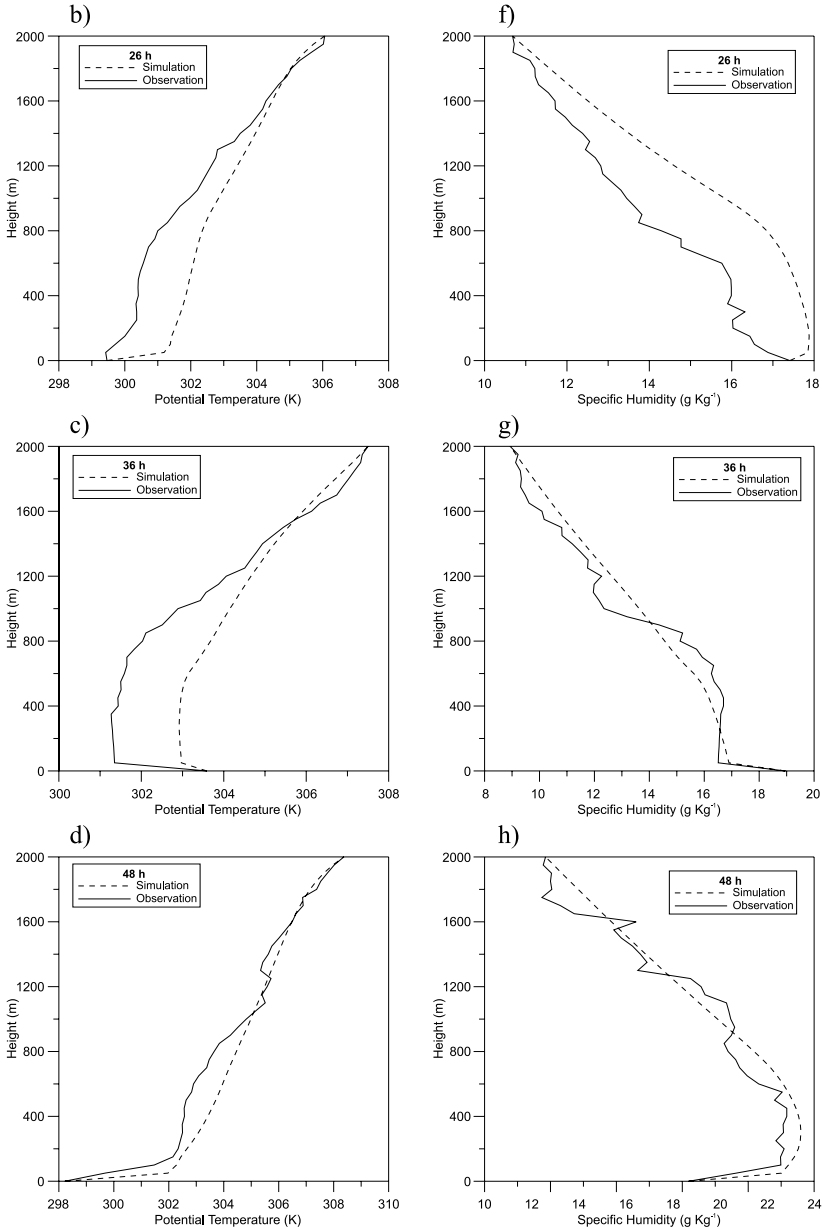


Fig. 9a-h. Vertical profiles of simulated and observed potential temperature (θ) and specific humidity (q) at different hours of simulations during case-II.

Table 2. Statistical evaluation of the model performance in simulating the zonal wind (u , ms^{-1}), meridional wind (v , ms^{-1}), potential temperature (θ , K) and specific humidity (q , g kg^{-1})

Simulation hours for case I/ case II	Variables	Case I		Case II	
		RMS Error	Cor. Coeff.	RMS Error	Cor. Coeff.
12/13	u	0.59	0.80	2.68	0.71
	v	1.74	0.69	2.92	0.20
	θ	0.06	0.98	0.45	0.94
	q	0.20	0.97	0.37	0.93
24/26	u	5.40	0.67	4.6	0.29
	v	2.28	0.73	3.41	0.37
	θ	0.05	0.98	0.82	0.98
	q	0.90	0.97	1.44	0.95
36/36	u	1.45	0.89	1.31	0.93
	v	3.51	0.09	3.31	0.30
	θ	0.93	0.97	0.82	0.98
	q	1.48	0.91	0.15	0.98
48/48	u	0.59	0.93	2.69	0.54
	v	1.08	0.33	0.01	0.54
	θ	1.76	0.96	0.39	0.98
	q	0.31	0.98	0.32	0.97
60/-	u	1.01	0.81		
	v	1.53	0.62		
	θ	1.66	0.97		
	q	1.31	0.97		

during the convectively active case than in the suppressed case. The growth in the PBL and the sudden rise in the H and LE during the convectively active case determine the dynamics and thermodynamical character of the convection processes. The temporal variation of TKE evolution show higher values during active convection case as compared to the suppressed case. The 1-D simulation of the surface fluxes of H and LE, the PBL height and the TKE correlate well with both the synoptic conditions studied.

The 1-D model simulation of vertical profiles of θ and q are found to be in good agreement with the observations as a validation of the high-resolution upper air data, obtained for the first time at Goa. However, the model simulations of u and v wind show deviations depicting that the thermodynamic structure was better reproduced than the dynamical fields in the simulation. Therefore, for a better simulation of the boundary layer using a 1-D model, it is important to have the advection terms incorporated in a

proper manner. However, the overall performance of the 1-D model is fairly promising. It can be therefore noted that such a model with refinement can be used as a tool in data-sparse regions along with available soundings to generate time-varying representative profiles that are comparable with the observations. These simulated values can be used to enhance the analysis of a 3-D model, which along with a mesoscale model can be used to study the transport and entrainment processes over the region.

Acknowledgments. The authors wish to sincerely acknowledge the Department of Science and Technology (DST) Govt. of India for providing necessary funds through the SERC-Fast Track Young Scientist (FTYS)-program (SR/FTP/ES-019/2003) and the Centre for Atmospheric Sciences, Indian Institute of Technology, Delhi for providing required facilities to carry out this work. We sincerely thank NOAA/ESRL, PSD (NCEP/NCAR), USA and EUMETSAT for making available the plots and satellite imageries, respectively. N. V. Sam is gratefully acknowledged for his kind co-operation in the work. The authors acknowledge the ARMEX Scientific team for providing the necessary data for the present study. We also thank the editor and referee for their helpful comment and suggestions which contributed to an improved version of the final manuscript.

References

- Augstein E., Riehl H., Ostapoff F., Wagoner V., 1971: Mass and energy transports in an undisturbed Atlantic trade wind flow. *Mon. Wea. Rev.* **101**, 101–111.
- Bagavath A. S., Venkatesan R., Srinivasan C. V., Somayaji K. M., 2005: Atmospheric boundary layer observations on the East coast at Kalpakkam using Doppler minisodar during different seasons. *Mausam*, **56**, 1, 233–242.
- Basu S., Raman S., Mohanty U. C., Rajagopal E. N., 1999: Influence of Planetary boundary layer physics on the medium-range prediction of the monsoon over India. *Pure and Applied Geophysics*, **155**, 33–55.
- Bhat G. S., 2003: Some salient features of the atmosphere observed over the North Bay of Bengal during BOBMEX. *Proc. Indian. Acad. Sci., Earth Planet. Sci.*, **112**, 131–146.
- Bhat G. S., Chakraborty A., Nanjundiah R. S., Srinivasan J., 2002: Vertical thermal structure of the atmosphere during active and weak phases of convection over the north Bay of Bengal: Observation and model results. *Curr. Sci.*, **83**, 296–302.
- Bhat G. S., Gadgil S., Hareesh Kumar P. V., Kalsi S. R., Madhusoodan P., Murty V. S. N., Prasada Rao C. V. K., Ramesh Babu V., Rao L. V. G., Rao R. R., Ravichandran M., Reddy K. G., Sanjeeva Rao P., Sengupta D., Sikka D. R., Swain J., Vinaychandran P. N., 2001: BOBMEX: The Bay of Bengal Monsoon Experiment. *Bull. Amer. Meteor. Soc.*, **82**, 2217–2243.

- Das Y., 2004: The role of oceanic heat content and mixed layer characteristics in simulating air-sea fluxes and MBL characteristics over Indian Ocean using 1-D PBL model (SR/FTP/ES-019/2003; 24/3/04).
- DST 1998: Indian Climate Research Programme Implementation plan. Department of Science and Technology, Govt. of India, New Delhi.
- Holland J. S., Rasmusson B. M, 1973: Measurements of the atmospheric mass, energy and momentum budgets over a 500 kilometer square of tropical ocean. *Mon. Wea. Rev.*, **101**, 44–55.
- Holt T., Raman S., 1987: A review and comparative evaluation of multilevel boundary layer parameterisations for first-order and turbulent kinetic energy closure schemes. *Rev. Geophys.*, **26**, 761–780.
- IMD 2002: Southwest monsoon – end of season report. India Meteorological Department, 10 p.
- Kloesel K. A, Albrecht B. R., 1989: Low-level inversions over the tropical pacific – thermodynamic structure of the boundary layer and the above-inversion moisture structure. *Monthly Weather Review*, **117**, 87–101.
- Kolmogorov A. N., 1942: *Izv. Akad. Nauk SSSR Ser. Fiz.* (Russia), 6, 56 p.
- Kusuma G. R., Raman S., Prabhu A., 1991: Boundary-layer heights over the monsoon trough region during active and break phases. *Bound. Layer Meteor.*, **57**, 129–138.
- Lykossov V. N., Platov G. A., 1992: A Numerical Model of Interaction between Atmospheric and Oceanic Boundary Layers. *Russ. Numer. Anal. Math. Modelling*, **7**, 419–440.
- Mohanty U. C., Sam N. V., Das S., Satyanarayana A. N. V., 2003: A Study on the Structure of the Convective Atmosphere over the Bay of Bengal during BOBMEX-99. *Proc. Indian Acad. Sci., Earth Planet. Sci.*, **112**, 147–163.
- Mohanty U. C. et al., 2002: Weather Summary during ARMEX-2002 (Report).
- Mohanty U. C., Sam N. V., Satyanarayana A. N. V., 2002: Simulation of marine boundary layer characteristics over the Indian ocean during INDOEX-IFP'99. *Indian Journal of Radio and Space Physics*, **31**, 376–390.
- Mahanty U. C., Sam N. V., Das S., Basu S., 2005: A study on the convective structure of the atmosphere over the West Coast of India during ARMEX-I. *Mausam*, **56**, 1, 49–58.
- Potty K. V. J., Mohanty U. C., Raman S., 1997: Effect of three different boundary-layer parameterisations in a regional atmospheric model on the simulation of summer monsoon circulation. *Bound. Layer Meteor.*, **84**, 363–381.
- Sam N. V., Mohanty U. C., Basu S., Prasad Rao A. K. S. A. V., 2003a: A study of the boundary layer characteristics and associated convective processes over the west coast of India during ARMEX-2002. *Proceedings of ARMEX workshop, 22-23 Dec., 2003, NIOT, Chennai, India*, 48 p.
- Sam N. V., Mohanty U. C., Satyanarayana A. N. V., 2003b: Simulation of Marine Boundary Layer Characteristics using a 1-D PBL model Over the Bay of Bengal during BOBMEX-99. *Proc. Indian Academy of Sciences*, **112**, 2, 185–204.

- Sam N. V., Mohanty U. C., Kaur P. S., 2005: Conserved variable and observational analysis over the West coast of India during ARMEX-2002. *Mausam*, **56**, 1, 201–212.
- Satyanarayana A. N. V., Mohanty U. C., Devdutta S. N., Raman S., Lykossov V. N., Warrior H., Sam N. V., 2001: A study on marine boundary layer processes in the ITCZ and non-ITCZ regimes over Indian Ocean with INDOEX IFFP-99 data. *Curr. Sci.*, **80**, 10, 39–45.
- Satyanarayana A. N. V., Mohanty U. C., Sam N. V., Basu S., Lykossov V. N., 2000: Numerical simulation of the marine boundary layer characteristics over the Bay of Bengal as revealed by BOBMEX-98 Pilot Experiment. *Proc. Indian Acad. Sci., Earth Planet. Sci.*, **109**, 293–303.
- Satyanarayana A. N. V., Mohanty U. C., Sam N. V., 1999: A study on the characteristics of the marine boundary layer over Indian Ocean with ORV Sagar Kanya cruise # 120 during 1997. *Curr. Sci.*, **76**, 890–897.
- Satyanarayana A. N. V., Lykossov V. N., Mohanty U. C., Machufuskaya E. E., 2003: Parametrization of land surface processes to study boundary layer characteristics over semiarid region Gujarat, North West India. *J. Appl. Meteorol.*, **42**, 4, 528–540.
- Shao Y., Hacker Jorg M., Schwerdtfeger P., 1991: The structure of turbulence in a coastal atmospheric boundary layer. *Quarterly Journal of the Royal Meteorological Society*, **117**, 1299–1324.
- Sommeria G., Lemone M. A., 1978: Direct testing of a three-dimensional numerical model of the planetary boundary layer against experiment data. *Jour. Atmos. Sci.*, **35**, 25–39.
- Tjernström M., Smedman A.-S., 1993: The vertical turbulence structure of the coastal marine atmospheric boundary layer. *J. Geophys. Res.*, **98**, C3, 4809–4832.
- Warrior H., 1999: M. S. thesis. Department of Marine, Earth, Atmospheric Sciences, North Carolina State University, Raleigh NC, USA.